
**Liquid Crystals**
Publication details, including instructions for authors and subscription information:
http://www.informaworld.com/smpp/title~content=t713926090

# Shear flow induced deformations of planar cholesteric layers

Grzegorz Derfel; Dariusz Krzyzanski

Online publication date: 06 August 2010

**To cite this Article** Derfel, Grzegorz and Krzyzanski, Dariusz(1997) 'Shear flow induced deformations of planar cholesteric layers', Liquid Crystals, 22: 4, 463 — 468
**To link to this Article: DOI:** 10.1080/026782997209180
**URL:** http://dx.doi.org/10.1080/026782997209180

LIQUID CRYSTALS, 1997, VOL. 22, NO. 4, 463–468

# Shear flow induced deformations of planar cholesteric layers

by GRZEGORZ DERFEL* and DARIUSZ KRZYZAŃSKI
Institute of Physics, Technical University of Łódź, ul. Wólczańska 223,
93-005 Łódź, Poland

(*Received 11 July 1996; in final form 11 November 1996; accepted 6 December 1996*)

The shear flow induced deformation of the planar cholesteric structure is modelled numerically, taking into account long pitch flow-aligning material. Three pitch-to-thickness ratios in five configurations are considered. Unwinding of the cholesteric helix due to the flow alignment is found. This process has a threshold character, when the mid-plane director is perpendicular to the plane of shear; otherwise it is continuous. The transverse component of the flow is always present. At high stress, the director in the prevailing part of the layer is oriented at the flow-aligning angle.



## 1. Introduction

The coupling between the director and the velocity gradient gives rise to a viscous torque which deforms the initial structure of liquid crystals. In cholesterics, the character of the deformation depends on the direction of the helical axis with respect to the velocity vector and velocity gradient. Briefly, three kinds of phenomena can be distinguished. In the case of the helical axis parallel to the velocity gradient (for instance in a sheared planar layer), unwinding of the chiral structure has been found [1, 2]. If the helical axis is parallel to the velocity, the permeation effect, which manifests itself by an enormous effective viscosity, takes place [3, 4]. If the helical axis is oriented perpendicular both to the velocity vector and to the velocity gradient, unwinding of the chiral structure occurs [5], analogously to the field induced cholesteric–nematic transition. The details of the deformations depend on the geometry of the flow.

In the present paper, simple shear flow of a long pitch cholesteric with the helical axis parallel to the velocity gradient is modelled numerically. A positive ratio of the Leslie viscosity coefficients $\alpha_3/\alpha_2$ is adopted. Director distributions are calculated for several pitch-to-thickness ratios and for various shear stresses. The calculations are performed for an infinite layer with strong boundary anchoring. The deformation is assumed to be one-dimensional; thermomechanical coupling is ignored. The deformation takes the form of unwinding of the cholesteric helix. High shear stress leads to a flow induced uniform director distribution as found usually for the flow-aligning nematics [6, 7]. The sheared chiral structure gives rise to transverse flow.

A similar problem was studied by Kini [1, 2], where the director orientations, velocity profiles and apparent viscosity were studied analytically and numerically as functions of pitch and shear rate. The results obtained in the present work agree qualitatively with Kini's results.

In addition to the unwinding and to the nematic-like flow induced orientation, threshold behaviour of the deformation is found. It takes place if the midplane director is normal to the plane of shear. The unwinding increases rapidly above some critical shear stress.

## 2. Method

The cholesteric liquid crystal is described by the elastic constant ratios $k_t = k_{22}/k_{11}$, $k_b = k_{33}/k_{11}$, the viscosity coefficient ratios $\alpha_i/\alpha_2$, $i = 1 \ldots 6$, and the pitch-to-thickness ratio $P/d$. A positive $\alpha_3/\alpha_2$ ratio is assumed, which is characteristic for flow aligning nematics. The material is confined in a layer of thickness $d$ between two plates parallel to the $xy$ plane and positioned at $z = \pm d/2$. The upper plate moves along the $y$ axis under the action of a constant shear stress $\tau$. The stationary director distribution in the deformed layer is described by two angles: the tilt angle, $\theta(z)$, between the director and its projection $n_{xy}$ on the $xy$ plane, and the azimuthal angle, $\phi(z)$, between $n_{xy}$ and the $y$ axis. The angle $\phi(z)$ is a measure of the director rotation about the $z$ axis. The angle $\theta(z)$ stands for the director rotation about another axis which is perpendicular to $\mathbf{n}$ and $n_{xy}$. Boundary conditions are determined by the strong anchoring, identical at both plates. Surface director orientation is determined by the easy axis versor $\mathbf{e}$, which lies in the $xy$ plane and makes the angle $\phi_s$ with the $y$ axis.

The stationary state in the sheared layer results from the equilibrium of the elastic and viscous torques in the bulk, and the elastic, viscous and surface torques at the

*Author for correspondence.

boundaries. The formulae for these torques are derived by use of Ericksen–Leslie theory [7]. They are gathered in the Appendix.

In our computer model, the continuous $\theta(z)$ and $\phi(z)$ functions are replaced by the sets of $N$ discrete values $\theta_i$ and $\phi_i$ determined in $N$ equidistant planes positioned at $z_i = -d/2 + (i-1)d/(N-1)$, where $i = 1 \ldots N$. The values $\theta_i$ and $\phi_i$ are used for the calculation of the torques per unit volume, which affect the director in the sublayers attached to each of the $N$ planes. (There are $N$ sublayers; the two sublayers that are adjacent to the boundary plates have a thickness equal to $d/[2(N-1)]$, and all others, which are in the bulk, have the thickness $d/(N-1)$.) For each of the inner sublayers, the sum of the elastic and viscous torques is calculated, while for the boundary sublayer, the third torque due to the surface anchoring is added.

The equilibrium set of angles $\theta_i$ and $\phi_i$, which approximates the real stationary director distribution, is calculated in the course of an iteration process. The initially adopted values $\theta_i$ and $\phi_i$ (corresponding to the undeformed layer) are varied sequentially. The new values are accepted if they give a smaller absolute value $|\Gamma_i|$ of the torque per unit volume in the $i$-th sublayer. This procedure is repeated until the sum of all $|\Gamma_i|$ decreases below some sufficiently low value $\varepsilon$ due to the required accuracy. (In our calculations $\varepsilon = 10^{-4}$ while $N = 64$, which gives satisfactory approximations of the continuous $\theta(z)$ and $\phi(z)$ functions.)

## 3. Results

The parameters of the material correspond to the nematic liquid crystal APAPA: $k_t = 0{\cdot}565$, $k_b = 1{\cdot}59$, $\alpha_1/\alpha_2 = -0{\cdot}1$, $\alpha_3/\alpha_2 = 0{\cdot}149$, $\alpha_4/\alpha_2 = -0{\cdot}795$, $\alpha_5/\alpha_2 = -1{\cdot}385$, $\alpha_6/\alpha_2 = -0{\cdot}234$. They are adopted from [8] and [9]. The left-handed cholesteric structure is assumed to derive from the chiral additive which does not change the parameters of the pure compound. Three pitch-to-thickness ratios are taken into account: $P/d = 4/3$, $P/d = 1$ and $P/d = 2/3$. The dimensionless parameter



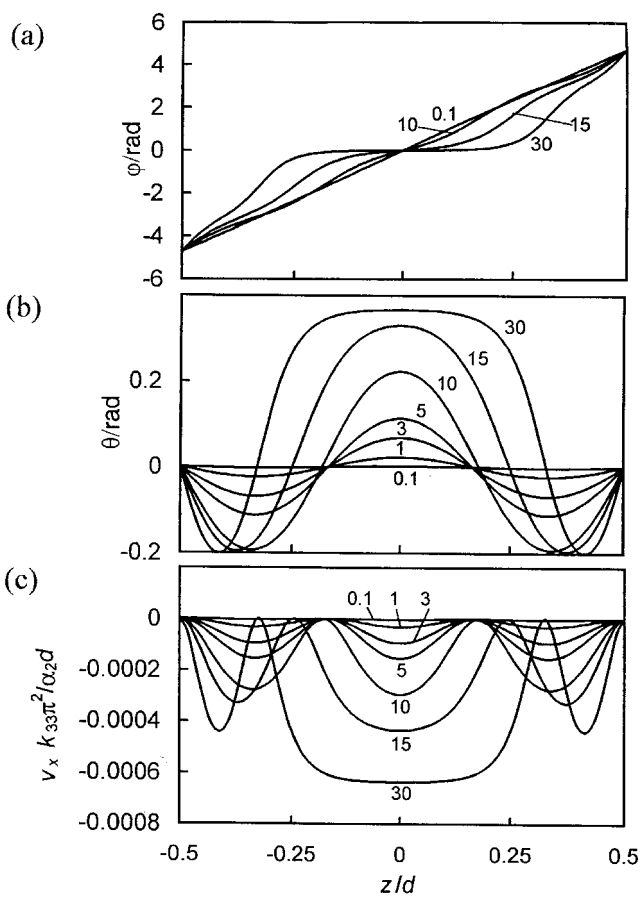


Figure 1. The smooth unwinding of the cholesteric structure for $\phi(z=0)=0$. $P=2d/3$; (*a*) the azimuthal angle $\phi(z)$; (*b*) the tilt angle $\theta(z)$; (*c*) the transverse velocity $v_x(z)$. The dimensionless stress values are indicated.

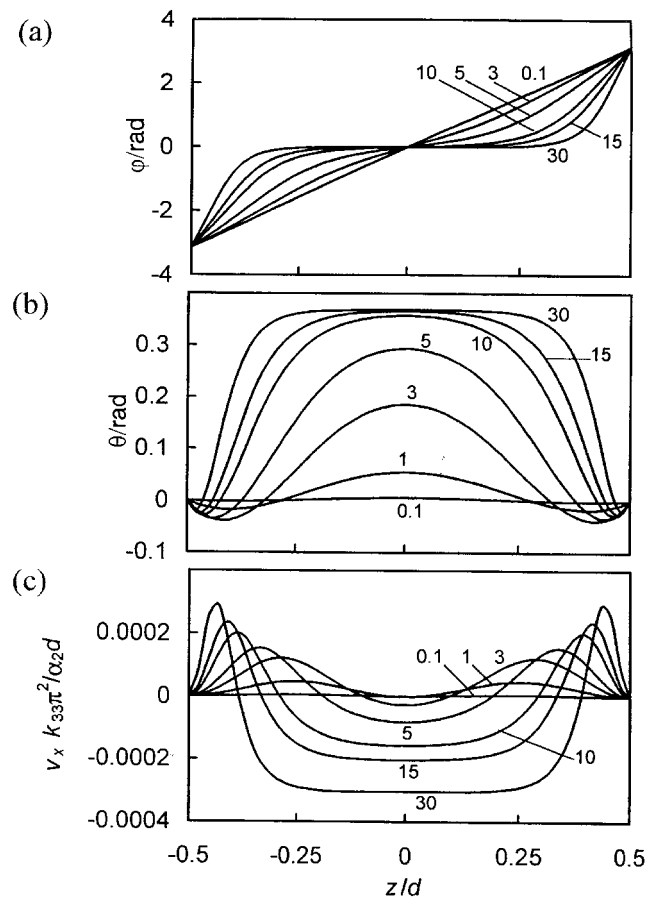


Figure 2. The smooth unwinding of the cholesteric structure for $\phi(z=0)=0$. $P=d$; (*a*) the azimuthal angle $\phi(z)$; (*b*) the tilt angle $\theta(z)$; (*c*) the transverse velocity $v_x(z)$. The dimensionless stress values are indicated.

$\gamma = Wd/k_{11}$, describing the anchoring strength, is chosen to be equal to $2 \times 10^5$. (The surface anchoring energy per unit area of the layer $W$ is defined by equation (A11).) The intrinsic pitch of the material matches the directions of the easy axes on both boundary plates. Two surface orientations are used: parallel and perpendicular to the shear plane. They give two configurations of the helical structures for each $P/d$ ratio with the exception of $P/d=4/3$. In the latter case, the easy axis is parallel to the plane of shear at $z=-d/2$, whereas it is perpendicular at $z=d/2$. As a result of this, five different situations arise. In each of them, the director distributions given by the angles $\phi(z)$ and $\theta(z)$, the transverse shear stress $\sigma$, the apparent viscosity $\eta$, and the longitudinal and the transverse velocity profiles $v_y(z)$ and $v_x(z)$ are determined as functions of the external shear stress $\tau$. The results are presented in dimensionless form, achieved by means of a suitable choice of units, namely, $d$ as the unit for distance, $\alpha_2$ for viscosity, $k_{33}\pi^2/\alpha_2 d$ for velocity and $k_{33}\pi^2/d^2$ for stress. In particular, the dimensionless stress $t=\tau d^2/\pi^2 k_{33}$ is used.

Deformations of the cholesteric structure can be interpreted as the effect of flow induced alignment. At high shear stress, the director in a significant part of the layer thickness is oriented parallel to the shear plane at the flow aligning angle $\theta_c=\arctan(\alpha_3/\alpha_2)^{\frac{1}{2}}$. This structure is formed as a result of unwinding of the cholesteric helix. The unwinding occurs in different ways depending on the director orientation in the midplane of the layer and on the pitch value. The twist is concentrated in rather thin regions adjacent to the boundary plates.

The regions, in which the unperturbed director is parallel to the $y$ axis are the natural sites where the helical structure starts to unwind. They correspond to the regions where $\phi=\pm m\pi$, ($m=0, 1, 2, \ldots$), except where $z=\pm d/2$. Figures 1 to 5 show that these regions expand when the stress increases. The unwinding is associated with enhanced twist in the neighbouring regions.

In configurations where $\phi(z=0)=0$, the unwinding starts wherever $\phi=\pm m\pi$ and proceeds smoothly with increasing stress, see figures 1 (*a*) and 2 (*a*). The director in the central part of the layer is aligned by the flow. For high stress, it lies in the shear plane and makes the angle $\theta_c$ with the $y$ axis, figures 1 (*b*) and 2 (*b*). The $\phi(z)$ function is odd and the $\theta(z)$ function is even. For small stress, $\theta=0$ wherever the director is normal to the plane of shear.

In the case of the longest pitch considered, $P=4d/3$, the asymmetry of the director distribution reflects the asymmetry of the surface orientation, see figures 3 (*a*) and 3 (*b*). The unwinding and flow alignment develop in the region where $\phi=\pi$.

In configurations where $\phi(z=0)=\pi/2$, the behaviour

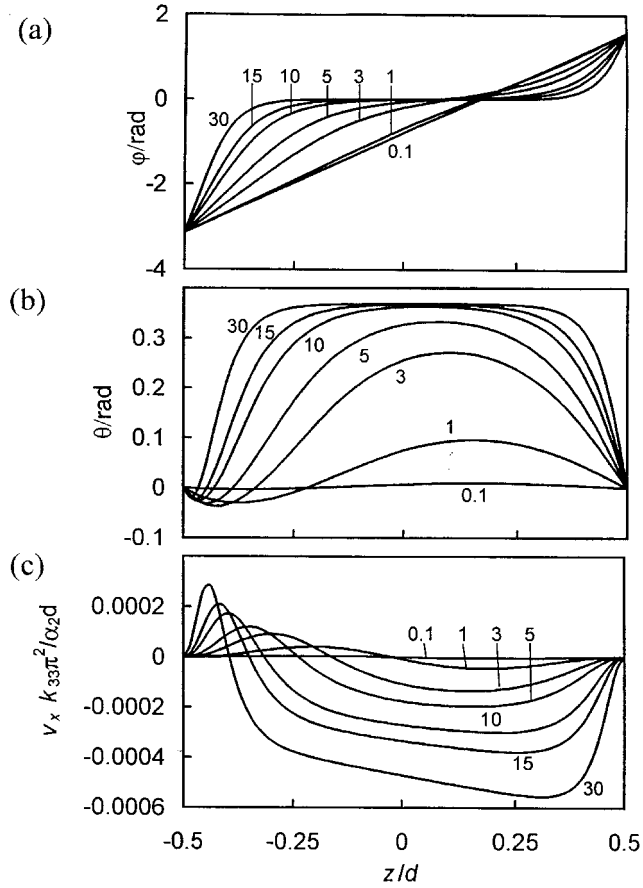


Figure 3. The smooth unwinding of the cholesteric structure for $P=4d/3$; (*a*) the azimuthal angle $\phi(z)$; (*b*) the tilt angle $\theta(z)$; (*c*) the transverse velocity $v_x(z)$. The dimensionless stress values are indicated.

of the layer is more interesting. The deformation occurs in two steps, as exemplified in figures 4 (*a*) and 5 (*a*). For small stress, weak unwinding arises for $\phi=0$ and $\phi=\pi$. The functions $\phi(z)-\pi/2$ and $\theta(z)$ are odd. When the stress exceeds some critical value, the director distribution changes abruptly, and the symmetry of the director profiles is broken. One of the regions, in which the unwinding is initialized, expands, while the unwinding in the other regions is damped. At higher stress, a significant part of the layer is aligned by the flow, see figures 4 (*b*) and 5 (*b*).

The high stress structures of all the five configurations are shown in figure 6, by means of cylinders, which symbolize the director.

The sheared twisted structure give rise to flow perpendicular to the shear plane. The transverse velocities are about two orders of magnitude lower than the longitudinal velocities. In configurations with $\phi(z=0)=0$, the profiles $v_x(z)$ are even, figures 1 (*c*) and 2 (*c*), as results from equation (A14). If $\phi(z=0)=\pi/2$, then the $v_x(z)$ are even only for sufficiently low stress. Above the critical

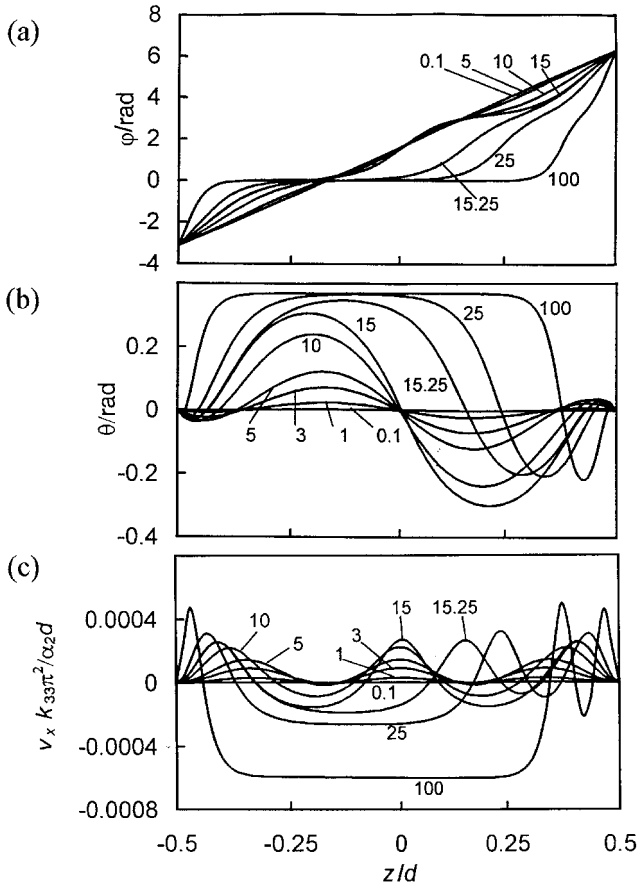


Figure 4. The threshold type unwinding of the cholesteric structure for $\phi(z=0)=\pi/2$, $P=2d/3$; (*a*) the azimuthal angle $\phi(z)$; (*b*) the tilt angle $\theta(z)$; (*c*) the transverse velocity $v_x(z)$. The dimensionless stress values are indicated.

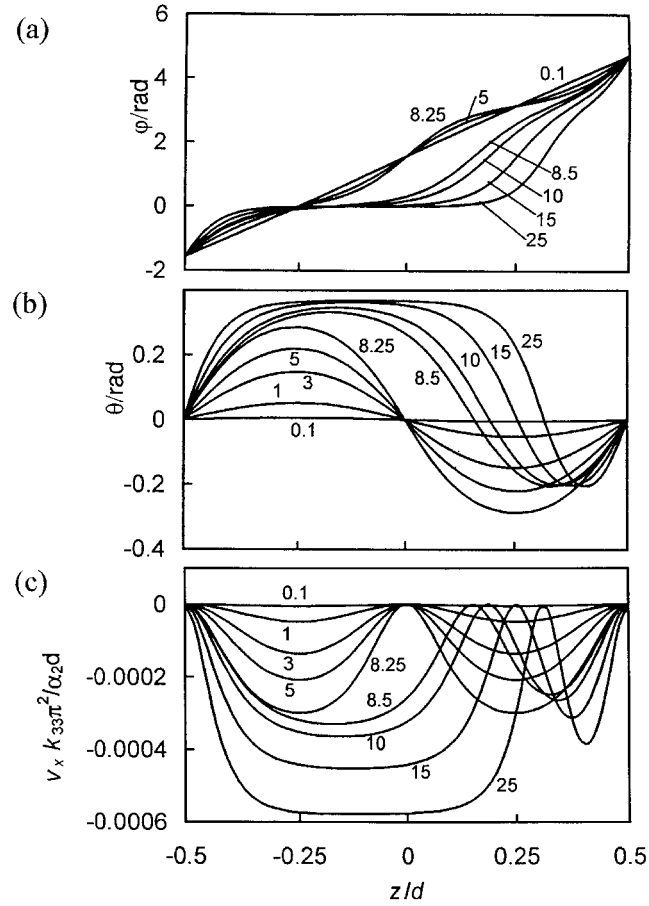


Figure 5. The threshold type unwinding of the cholesteric structure for $\phi(z=0)=\pi/2$, $P=d$; (*a*) the azimuthal angle $\phi(z)$; (*b*) the tilt angle $\theta(z)$; (*c*) the transverse velocity $v_x(z)$. The dimensionless stress values are indicated.



stress for unwinding, the symmetry is broken, figures 4(*c*) and 5(*c*). A similar lack of symmetry is observed for $P=4d/3$, figure 3(*c*).

Figure 7 shows the transverse shear stresses $\sigma$ plotted as functions of $t$ for the structures presented in figures 4 and 5. The threshold behaviour is very pronounced. The values of $\sigma$ for the asymmetric case of $P=4d/3$ increase monotonically and achieve a value of about 1·5 for $t=30$. For the structures with $\phi(z=0)=0$, the transverse stress vanishes, due to their symmetry.

Deformation of the structure of the layer influences the apparent viscosity, as illustrated in figure 8. The low stress viscosity coefficient is the same in all cases; it increases as a result of deformation, and tends to the value corresponding to the nematic aligned at the angle $\theta_c$. For the material constants adopted here, this limit value is greater than the initial viscosity of the undeformed layers. For given $t$, the increase is more pronounced for materials with longer pitch, which are more easily unwound than the more strongly twisted structures. Small jumps of the effective viscosity coefficient correspond to abrupt unwinding above the threshold stress.

The longitudinal velocity profiles are monotonic functions of $z$, as exemplified in figure 9.

## 4. Discussion

The director distributions and velocity profiles presented here agree qualitatively with the results reported in [1] and [2]. The threshold character of the deformation is revealed, which to our knowledge has not been reported earlier. This effect is analogous to field induced deformations in liquid crystals. The perpendicularity of the midplane director to the driving force of the distortion is the feature common to both phenomena.

In most cases considered here, the transverse velocity components have a unique sign in the whole layer; the transverse flow has a unique direction. The non-vanishing net flow is common in our results and in the results of [1] and [2]. The calculated director distributions correspond therefore to situations in which the

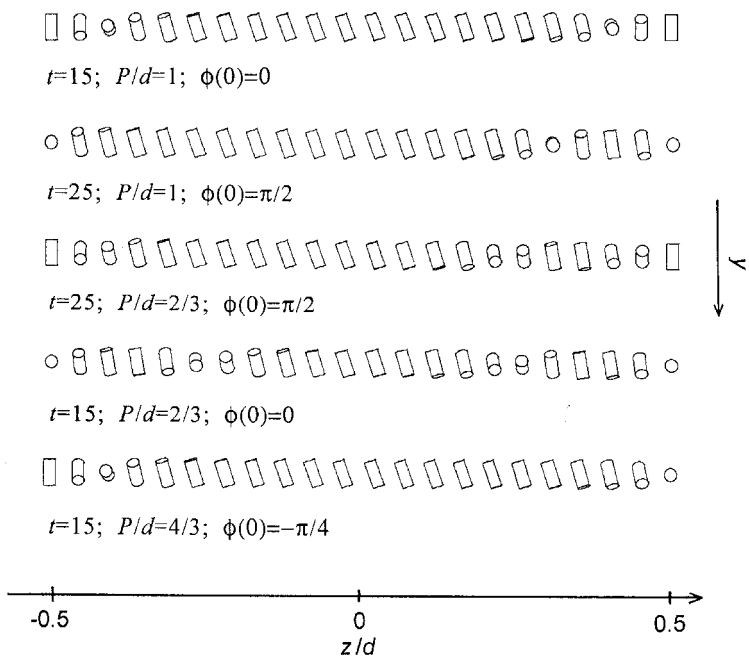


Figure 6. The unwound structure of the cholesteric layers at high stresses.



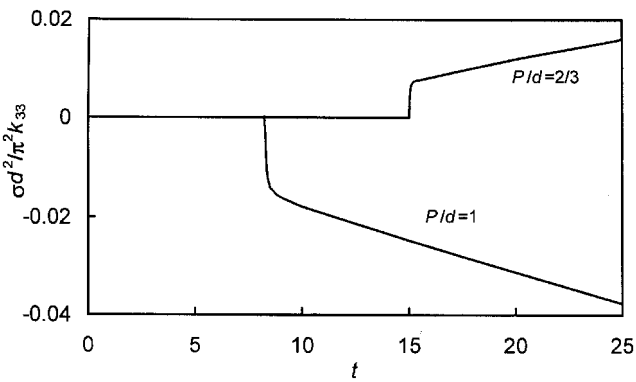


Figure 7. The transverse stress $\sigma$ as a function of the longitudinal stress $t$ for the threshold type unwinding of the cholesteric structure. The pitch to thickness ratios are indicated.

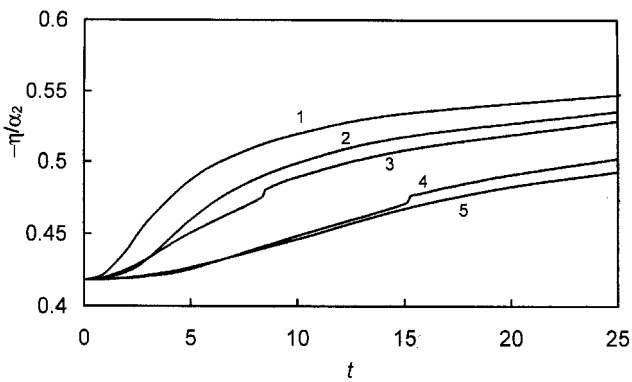


Figure 8. The effective viscosity $\eta$ as a function of the longitudinal stress $t$. 1: $P/d=4/3$; 2: $P/d=1$, $\phi(z=0)=0$; 3: $P/d=1$, $\phi(z=0)=\pi/2$; 4: $P/d=2/3$, $\phi(z=0)=\pi/2$; 5: $P/d=2/3$, $\phi(z=0)=0$.

liquid crystal has freedom of movement in the $x$ direction. Experimental realization of such flow may be troublesome; however, transverse velocities are about two orders of magnitude smaller than the longitudinal, and their influence on the director distribution is negligible. The transverse effects can be ignored and the results obtained here can be treated as adequate for experiments in which lateral boundaries prevent the transverse flow.

Summarizing, viscous torque affects the intrinsic twist of the cholesteric liquid crystal. The unwinding can have a threshold character, and the unwound structure is aligned by the flow, as for a nematic liquid crystal.

## Appendix

The director distribution in the stationary state in the sheared layer results from the equilibrium of the elastic and viscous torques in the bulk, and the elastic, viscous and surface torques at the boundaries.

The elastic torque is

$$\Gamma_{\text{elastic}} = \mathbf{n} \times \mathbf{h} \tag{A1}$$

where $\mathbf{n}$ is the director and $\mathbf{h}$ is the molecular field. Its components are given by

$$h_j = \frac{\partial g}{\partial n_j} - \frac{\partial}{\partial z}\frac{\partial g}{\partial n_{j,z}} \tag{A2}$$

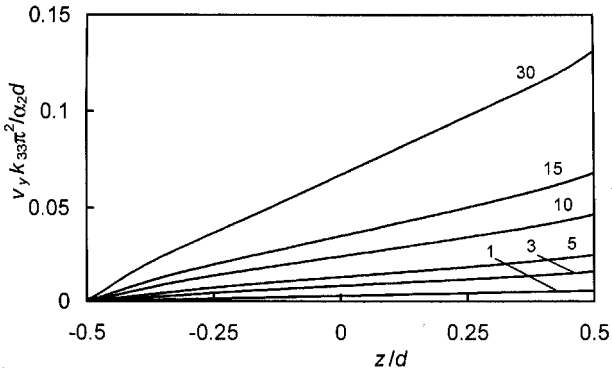


Figure 9. The longitudinal velocity profile $v_y(z)$ for $P/d=4/3$. The dimensionless stress values are indicated.

where $g$ is the Frank elastic free energy density and $n_{j,z}=\partial n_j/\partial z$ and $j=x, y, z$.

The viscous torque is expressed by the viscous force $\mathbf{f}'$:

$$\mathbf{\Gamma}=\mathbf{n}\times\mathbf{f}' \tag{A3}$$

The components of $\mathbf{f}'$ are

$$\begin{aligned} f'_x &= \alpha_2 w n_z \\ f'_y &= \alpha_2 u n_z \\ f'_z &= \alpha_3(u n_y + w n_x) \end{aligned} \tag{A4}$$

where $u=\partial v_y/\partial z$ and $w=\partial v_x/\partial z$. The velocity gradients $u$ and $w$ are given by the Navier–Stokes equations

$$\begin{aligned} \tau &= uP+wQ \\ \sigma &= uQ+wR \end{aligned} \tag{A5}$$

where

$$P=\frac{1}{2}\left[2\alpha_1 n_y^2 n_z^2+(\alpha_5-\alpha_2)n_z^2+(\alpha_3+\alpha_6)n_y^2+\alpha_4\right] \tag{A6}$$

$$Q=\frac{1}{2}\left[2\alpha_1 n_x n_y n_z^2+(\alpha_3+\alpha_6)n_x n_y\right] \tag{A7}$$

$$R=\frac{1}{2}\left[2\alpha_1 n_x^2 n_z^2+(\alpha_5-\alpha_2)n_z^2+(\alpha_3+\alpha_6)n_x^2+\alpha_4\right] \tag{A8}$$

and $\sigma$ is the transverse shear stress appearing if the director deviates from the shear plane, *i.e.* if $n_x\neq 0$ or $\phi\neq 0$. The value of $\sigma$ is determined by the 'no slip condition'

$$\int_{-d/2}^{d/2} w\,\mathrm{d}z=0 \tag{A9}$$

which leads to

$$\sigma=\tau\frac{\displaystyle\int_{-d/2}^{d/2}\frac{Q}{\Delta}\,\mathrm{d}z}{\displaystyle\int_{-d/2}^{d/2}\frac{P}{\Delta}\,\mathrm{d}z} \tag{A10}$$

where $\Delta=PR-Q^2$.

The anchoring free energy per unit area of the layer is assumed in the Rapini–Papoular form [10]

$$F_{\text{anchoring}}=-(W/2)(\mathbf{n}\cdot\mathbf{e})^2 \tag{A11}$$

where $\mathbf{e}$ is the surface easy axis versor.

The surface torque is expressed by

$$\mathbf{\Gamma}_{\text{anchoring}}=W(\mathbf{n}\cdot\mathbf{e})(\mathbf{n}\times\mathbf{e}) \tag{A12}$$

The director distribution allows calculation of the effective viscosity coefficient

$$\eta=\frac{\tau d}{\displaystyle\int_{-d/2}^{d/2}\frac{\tau R-\sigma Q}{\Delta}\,\mathrm{d}z} \tag{A13}$$

and the velocity components

$$v_x(z)=\int_{-d/2}^{z}\frac{\sigma P-\tau Q}{\Delta}\,\mathrm{d}z \tag{A14}$$

$$v_y(z)=\int_{-22}^{z}\frac{\pi R-\sigma Q}{\Delta}\mathrm{d}z \tag{A15}$$

## References


[1] Kini, U. D., 1979, *J. Phys., Paris*, **40,** C3–62.
[2] Kini, U. D., 1980, *Pramana*, **14,** 463.
[3] Goosens, W. J. A., 1981, *Phys. Lett. A*, **85,** 231.
[4] Sakamoto, K., Porter, R., and Johnson, J., 1969, *Mol. Cryst. liq. Cryst.*, **8,** 443.
[5] Derfel, G., 1983, *Mol. Cryst. liq. Cryst. Lett.*, **92,** 41.
[6] Gahwiller, C., 1972, *Phys. Rev. Lett.*, **28,** 1554.
[7] Leslie, F. M., 1979, *Adv. liq. Cryst.*, **4,** 1.
[8] Leenhouts, F., and Dekker, A. J., 1981, *J. chem. Phys.*, **74,** 1956.
[9] Van der Meulen, J. P., and Zijlstra, R. J. J., 1985, *Physica B*, **132,** 153.
[10] Rapini, A., and Papoular, M., 1969, *J. Phys. Colloq.*, **C-4,** 54.